



Preparation and characterization of TiO₂/ZnO/CuO nanocomposite and application for phenol removal from wastewaters

M. Mohammadi^a, S. Sabbaghi^{a,*}, H. Sadeghi^a, M.M. Zerafat^a, R. Pooladi^b

^aFaculty of Advanced Technologies, Nano Chemical Engineering Department, Shiraz University, Shiraz, Iran, Tel. +98 9171073830; email: mojtabamohammadi17@yahoo.com (M. Mohammadi), Tel. +98 9171133471, +98 7116133709; Fax: +98 7116286421; email: sabbaghi@shirazu.ac.ir (S. Sabbaghi), Tel. +98 9179076091; email: hasansadeghi89@gmail.com (H. Sadeghi), Tel. +98 9173100957; email: mmzerafat@shirazu.ac.ir (M.M. Zerafat)

^bNanotechnology Research Institute, Shiraz University, Shiraz, Iran, Tel. +98 9171135782; email: pooladi@shirazu.ac.ir (R. Pooladi)

Received 29 January 2014; Accepted 18 September 2014

ABSTRACT

The TiO₂/ZnO/CuO nanocomposite is prepared using mechanical mixing and wet impregnation under low-temperature conditions and characterized by scanning electron microscopy. The results indicate that the TiO₂/ZnO/CuO nanocomposite exhibits an appreciable photo-catalytic activity, which can mainly be attributed to the extended photo-responding range and the increased charge separation rate. Phenol removal is also measured as a function of irradiation time by using UV–vis spectrophotometer. The results show that phenol removal takes place more effectively in the presence of the nanocomposite under solar irradiation in comparison with UV irradiation. The influence of several parameters has investigated on the photo-catalytic removal of phenol such as pH and various synthesis techniques. The results show that the degradation rate decreases by increasing the pH value. The highest degradation rate is observed at 100 min after the beginning of the reaction and wet impregnation is proved to be more effective than mechanical mixing.

Keywords: Photo-catalytic removal; TiO₂/ZnO/CuO nanocomposite; UV irradiation; Solar irradiation

1. Introduction

Several studies have been conducted on different applications of metal oxide semiconductors for photo-catalytic environmental remediation such as wastewater decontamination, especially due to high photo-sensitivity, non-toxic nature, low cost, and environmental friendly characteristics [1–4]. However, there are some faults in the wide band gap semiconductors (such as TiO₂, CuO, and ZnO) as

photo-catalysts, since they can just be excited photo-catalytically under UV irradiation [5,6]. It is worth mentioning that, visible light with spectral wavelength in between 400 and 700 nm accounts for about 45% of the total solar radiation energy, while UV occupies <10% [7]. Thus, serious interest exists to improve the photo-catalytic activity for practical photo-catalytic applications under visible light. Besides, the fast recombination rate of the photo-generated electron-hole pairs in single-component semiconductors restricts their photo-catalytic efficiency [1]. The development of visible light-driven photo-catalysts with

*Corresponding author.

high energy-transfer efficiency, non-toxicity, and low cost is one of the most challenging tasks. Many efforts in photo-catalysis field are dedicated to the modification of the existing photo-catalysts in order to enhance their performance through different modification routes [8–10].

Among many candidates, TiO_2 has proven to be the most suitable choice for environmental applications because of biological and chemical inertness, stability against photo- and chemical corrosion, and also cost effectiveness [2–4]. Photo-excitation of TiO_2 with a light energy matching its band gap results in the production of electron–hole pairs. Photo-generated electrons and holes can migrate to the surface and react with the adsorbed reactants through the desired redox process or they may undergo undesired recombination, dissipating the input energy as heat. The photo-catalytic efficiency depends on the competition between these two processes namely, the ratio of surface charge carrier transfer to the electron–hole recombination rate. In order to increase the quantum yield, photo-induced electrons and holes should be separated to suppress recombination by utilizing a suitable surface defect state as a temporal trap [11].

Several contaminants are found in industrial wastewaters, among which phenol can be considered among the most harmful species for environmental and human health. Phenol can find way into wastewaters from different industrial sources like petroleum refineries, phenolic resins, formaldehyde resins, caprolactam textile, and some pharmaceutical processes. Due to toxicity and difficult degradation, the presence of phenol can become a considerable threat to the environment and human health [12,13]. Thus, phenol concentration in standard surface waters is limited to <1 ppb by environmental protection agency [14].

In order to remove phenolic compounds, different methods have been proposed and applied, such as chlorination, adsorption, and incineration. Chlorination can always be problematic since it generates carcinogenic byproducts [15,16]. Incineration of organic wastes is not always effective and can release large quantities of toxic compound emissions, such as products of incomplete combustion as well as heavy metal oxides into the atmosphere [17,18]. An ideal waste treatment process should completely degrade all toxic species present in the waste stream without leaving any hazardous residues [19]. Photo-catalysis, as one of the advanced oxidation processes (AOPs), involves the utilization of a comparatively non-toxic semiconductor photo-catalyst, especially titanium dioxide (TiO_2), in conjunction with light irradiation [1,20,21]. AOPs constitute a promising technology for the treatment of wastewaters containing biorecalcitrant compounds like

phenols. Some AOPs, such as UV photolysis [22], $\text{H}_2\text{O}_2/\text{UV}$ [23], ozone [24], ozone/UV, Fenton/UV [25], Fenton [26], and TiO_2/UV [27–29], have been studied for the decomposition of phenols. The UV light required may also come from an artificial source or sunlight [30–32].

In recent years, the heterogeneous photo-catalytic oxidation (HPO) employing TiO_2 and UV light has emerged as a novel promising route for the degradation of persistent organic pollutants, and for the production of more biologically degradable and less toxic substances [33,34]. This process is largely dependent on the *in situ* generation of hydroxyl radicals under ambient conditions capable of converting a wide spectrum of toxic organic compounds into relatively harmless end products such as CO_2 and H_2O . In the HPO process, the destruction of resistant organics is governed by the combined action of a semiconductor photo-catalyst, an energetic radiation source and an oxidizing agent. Moreover, the process can be driven by solar, UV, or visible light. Sunlight can produce $0.2\text{--}0.3$ mol photons $\text{m}^{-2} \text{h}^{-1}$ in the range of 300–400 nm with a typical $20\text{--}30$ W m^{-2} UV flux near the earth's surface which suggests sunlight as an economically and ecologically promising source for photo-catalytic degradation [35].

Due to the limitations involved on ensuring on effective photo-activation process, there has been a growing interest to go beyond the threshold wavelength (388 nm) corresponding to Titania band gap. The principle foci of these activities include:

- (1) incorporation of energy levels into Titania band gap,
- (2) changing the life time of charge carriers,
- (3) substitution of Ti^{4+} with a cation of the same size, and
- (4) shifting the conduction band and/or valence band so as to enable the photo-excitation at lower energies, the success of which depends on the preparation technique [36–38].

One of the effective methods to control TiO_2 surface properties is the introduction of semiconductor materials in its lattice structure. In this study, nanocrystalline TiO_2 particles are doped with CuO and ZnO semiconductor nanoparticles. The photo-catalytic behavior of the resulting powder is characterized by quantifying the degradation of phenol in aqueous suspensions in a fluidized bed photo-reactor. Preliminary experiments show that the prepared nanocomposite is more photo-active for phenol degradation in comparison with individual nanoparticles under visible light. The precursors for the prepared nanocomposite are

commercially available TiO_2 , zinc acetate, and copper nitrate. Therefore, the $\text{TiO}_2/\text{ZnO}/\text{CuO}$ nanocomposite is selected as the target material to be synthesized through a co-precipitation routine and further to investigate the photo-catalytic activity of multicomponent semiconductor systems. Based on these considerations, $\text{TiO}_2/\text{ZnO}/\text{CuO}$ nanocomposite is expected to show an enhanced photo-catalytic activity compared with single component CuO , ZnO , and TiO_2 nanocatalysts. The effect of various experimental parameters such as pH and synthesis routines have been investigated on the photo-catalytic phenol removal.

2. Materials and methods

2.1. Materials

The TiO_2 nanopowder with <30 nm particle size and $120 \text{ m}^2/\text{g}$ specific surface area is supplied by Technon Co. (Spain). Analytical reagents such as sodium hydroxide (NaOH), phenol, zinc acetate, copper nitrate, HCl, methanol, isopropanol, and ethanol are supplied by Merck. All chemicals were used without further purification. Deionized distilled water obtained from Millipore system was used in the preparation of solutions.

2.2. The experimental procedure

2.2.1. Synthesis of CuO nanoparticles

Copper acetate of 2.7 g and 2 ml of acetic acid are mixed with 600 ml of ethylene glycol in a flask equipped with a return mechanism, in order to prepare the CuO nanoparticles. Then, the solution is stirred vigorously by a hot plate stirrer. The solution is heated up to 78°C and 40 ml of NaOH (1 M) is gradually dropped into the solution under magnetic stirring at 78°C until the pH reaches up to 6–8, the point at which a considerable amount of dark-colored precipitate is observed. Being cooled at room temperature, the precipitate is centrifuged; the unwanted products are removed and CuO nanoparticles are purified, and the generated solution is washed several times with ethanol and deionized water [39–41].

2.2.2. Synthesis of ZnO nanoparticles

Zn $(\text{CH}_3\text{CO}_2)_2 \cdot \text{H}_2\text{O}$ of 0.10 g is dissolved in 25 ml of isopropanol by heating for 15 min and mixed with a 0.10 M NaOH solution in water, and rapidly stirred until it reaches pH of 12.12. The solution is heated in a 65°C paraffin bath during the experiment. After the reaction completion, the product is aged at room

temperature. Finally, the ZnO precipitates are separated and washed using deionized water and ethanol for three times [7]. The final product having a white-grayish color was dried in the oven at 65°C for 24 h.

2.2.3. Synthesis of $\text{TiO}_2/\text{ZnO}/\text{CuO}$ nanocomposite

2.2.3.1. Mechanical mixing. Mechanical mixing is used for the preparation of $\text{TiO}_2/\text{ZnO}/\text{CuO}$ nanocomposite. The oxide powders were mixed in ethanol with mortar for 15 min and were sonicated for 30 min. The amount of TiO_2 , ZnO, and CuO in the mixing process was 0.2, 0.05, and 0.05 g, respectively. An electric furnace was used for sintering at 550°C under the air

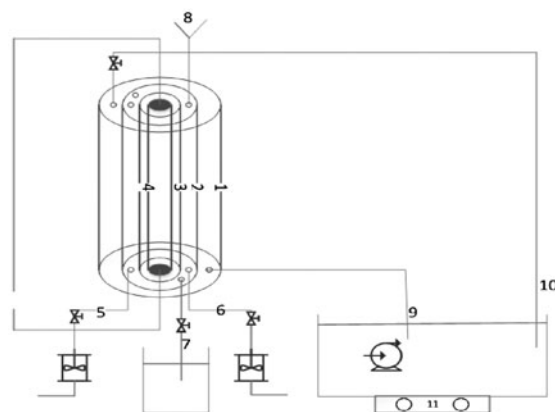


Fig. 1. The schematic of the photo-reactor used for phenol photo-catalytic degradation: (1) shell, (2) reaction zone, (3) quartz tube, (4) UV lamp, (5 and 6) input air, (7) sample output, (8) sample and catalyst input, (9 and 10) input and output of hot or cold water for controlling the temperature, and (11) heater stirrer.

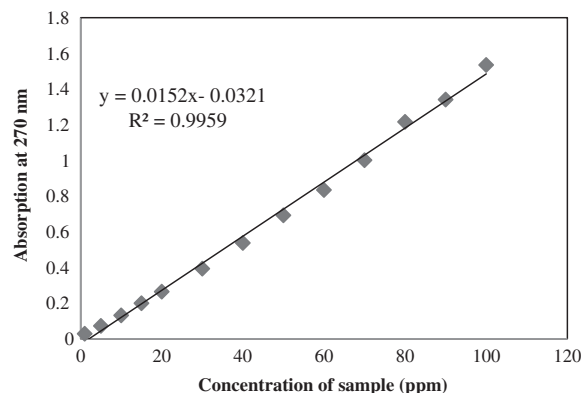


Fig. 2. Calibration curve for finding unknown phenol concentration.

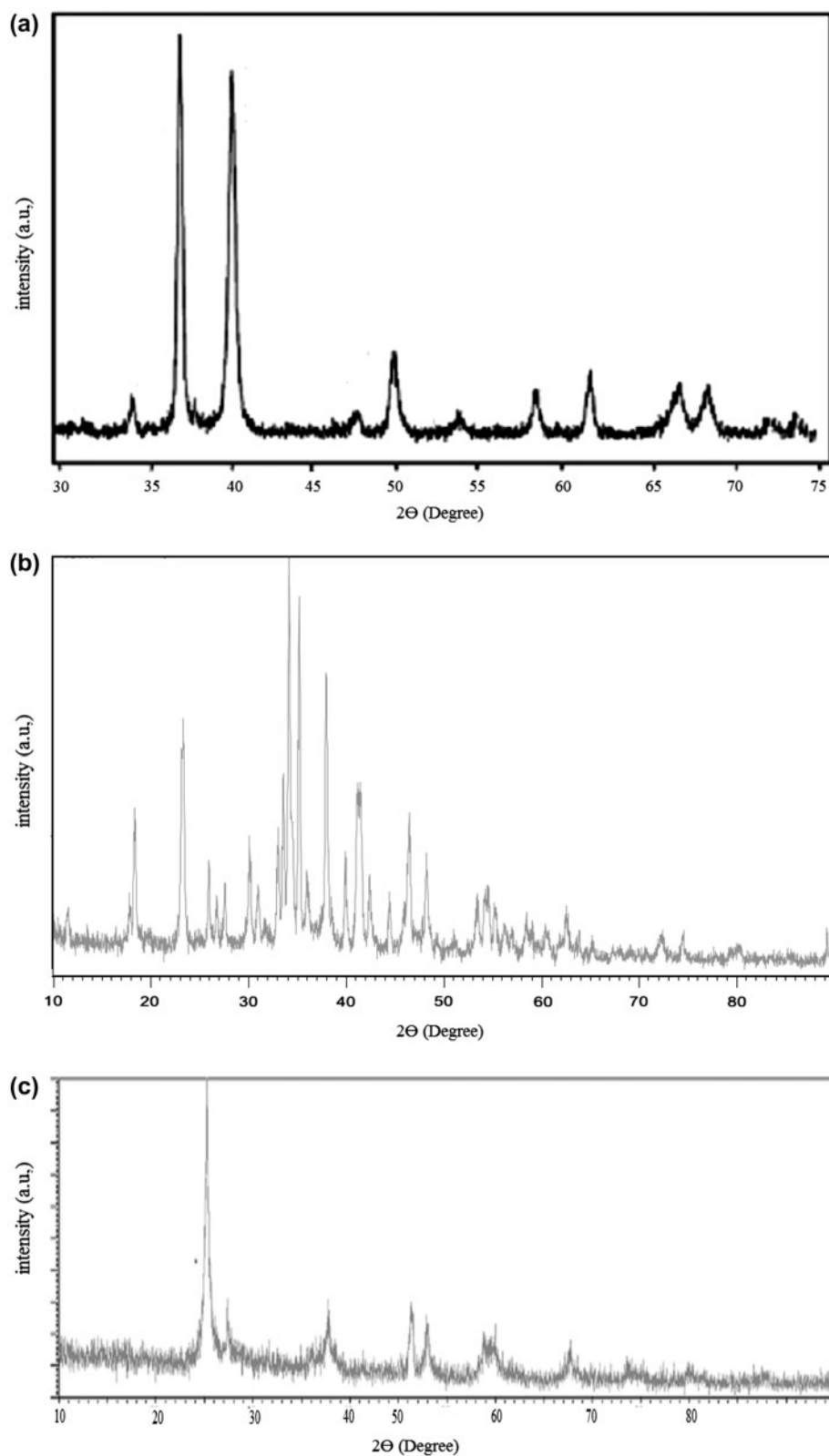


Fig. 3. XRD pattern of (a) CuO, (b) ZnO, (c) TiO_2 , (d) $\text{TiO}_2/\text{ZnO}/\text{CuO}$ nanocomposite from wet impregnation method, and (e) $\text{TiO}_2/\text{ZnO}/\text{CuO}$ nanocomposite from mechanical mixing method.

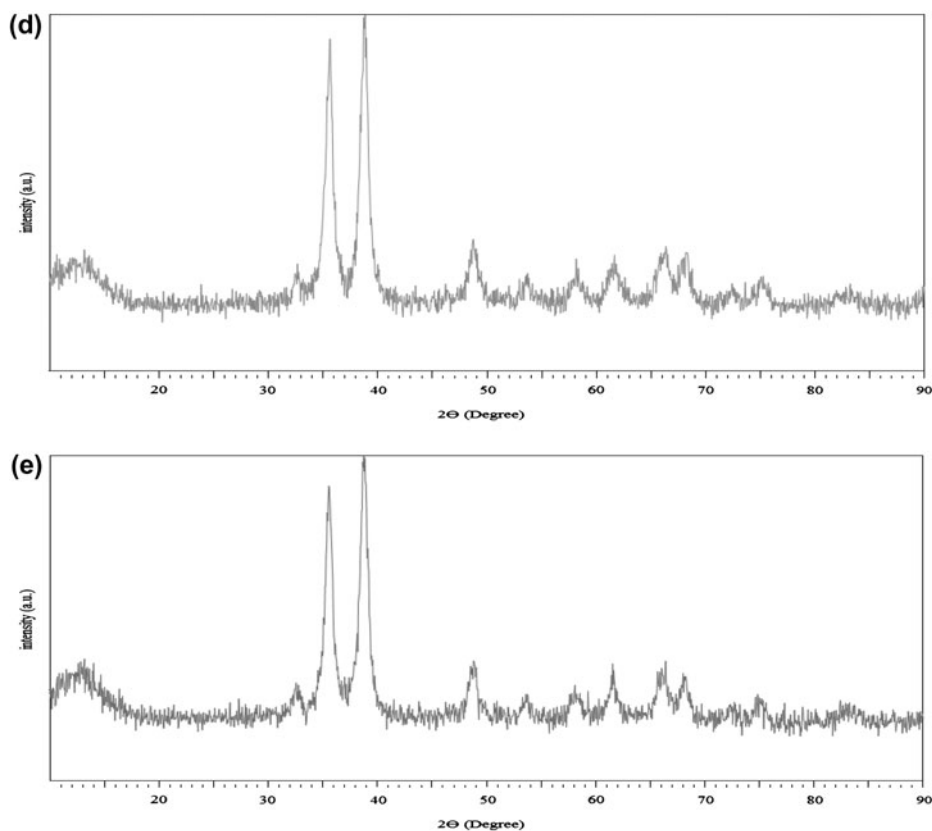


Fig. 3. (Continued).

atmosphere. The furnace was heated from the ambient to the final sintering temperature of 550°C at 4.7°C/min heating rate and then the temperature was kept constant for 3 h.

2.2.3.2. Wet impregnation. The TiO₂/ZnO/CuO photocatalyst was prepared through wet impregnation technique using TiO₂ nanopowder (Technon 20–25 nm). At first, 1 M solution of copper nitrate and zinc acetate were prepared (10 ml of copper nitrate and 10 ml of zinc acetate). After that, 0.2 g of TiO₂ was added to the solution under magnetic stirring. Ultrasonication was also applied for about 15 min with a 70 kHz power to obtain a homogeneous solution. Upon wet impregnation, the sample was dried at 105°C in the oven for 9 h and finally kept in a furnace at 550°C for 3 h, in order to remove the remaining impurities [8].

2.2.4. Apparatus

The experiments on the photo-catalytic degradation of phenol under solar and UV irradiation were performed in a batch photo-reactor (Fig. 1). The 1-l capacity cylindrical photo-reactor (height = 40 cm, ID

of the reaction zone = 6 cm, shell ID = 10 cm, and quartz tube ID = 2 cm) was made of Pyrex glass. The reaction temperature was maintained at 30°C using an outer shell. Inside the photo-reactor, an 8 W UV lamp is installed, surrounded by a quartz tube and placed at the center of the fluidized bed reactor. The lamp has a maximum intensity at a light wavelength of 254 nm. The solar irradiation experiment was carried out under solar light (Shiraz city at Iran, with the geographical longitude of 29.6167° N and 52.5333° E during 12–16).

2.2.5. Photo-catalytic degradation

Two hundred milliliters of a solution containing 50 ppm of phenol was transferred into the photo-reactor in the presence of a 200 ml/min flow of oxygen and left under agitation for 2 h. Then, 0.15 g of the prepared nanocomposite was introduced into the photo-reactor. The reaction was carried out at pH 5. A 10 ml sample of the reaction solution was collected every 1 h during the photo-oxidation to monitor the reduction of phenol concentration by using a UV-vis spectrophotometer (Jasco, model: V-530, USA)

performed under a scanning wavelength in the range of 190–900 nm. In order to use the UV–vis spectrophotometer, a number of phenol observant solutions with known concentrations (1, 5, 10, 15, 20, 30, 40, 50, 60, 70, 80, 90, and 100 ppm) were prepared. Based on the results, a graph of absorbance vs. concentration (calibration curve, Fig. 2) is obtained which results in 270 nm, which is the height of phenol observant. Phenol concentrations before and after photo-degradation were calculated from the calibration curve (Eq. (1)). The amount of absorbance at 270 nm is used to find the concentration of the phenol solution. The degree of phenol removal as a function of time is then given by Eq. (2):

$$(\text{Absorbance at } 270 \text{ nm}) = 0.0152 \times C(\text{ppm}) - 0.0321 \quad (1)$$

$$\text{Phenol removal } \% = \frac{C_0 - C}{C_0} \times 100 \quad (2)$$

where C_0 and C are phenol concentrations at the initial and the upcoming reaction times.

3. Results and discussion

3.1. Characterization and morphology of TiO_2 , ZnO , CuO , and $\text{TiO}_2/\text{ZnO}/\text{CuO}$ nanocomposite

3.1.1. X-ray diffraction

The composition of the samples were examined using unisantis XMD 300, X-ray diffractometer, and systematic Xpert PRO X-ray diffraction (XRD; $\lambda = 0.17890$ nm). The 2θ confine used was starting at 10–80 with 0.02 steps. No impurity peaks were observed in the XRD patterns. The broadening of the peaks indicates the small size of the products. Actually, the average size of the CuO and ZnO nanoparticles are estimated to be 4 and 5 nm according to the Scherrer equation [5]. Fig. 3(a)–(e) shows the XRD patterns of CuO , ZnO , TiO_2 , the nanocomposite from wet impregnation, and the nanocomposite from mechanical mixing, respectively.

3.1.2. Fourier transform infrared spectroscopy

Fourier transform infrared spectroscopy (FTIR) patterns of the ZnO , CuO , and TiO_2 are shown in Fig. 4(a)–(c), respectively.

Based on Fig. 4(a), the absorption peaks at 1,569 and $1,416 \text{ cm}^{-1}$ in the spectrum are due to the asymmetric and symmetric stretching vibrations of carbonyl

group (COO, Zn) in the zinc acetate, respectively. The main peaks at $\sim 500 \text{ cm}^{-1}$ corresponding to the (Zn, O) frequency modes confirm the formation of ZnO . The band centered at $\sim 3,436 \text{ cm}^{-1}$ is characteristic of O–H stretching and bending vibrations of H–O–H from the adsorbed water molecules.

Fig. 4(b) shows the FTIR spectrum of CuO nanoparticles. The peak at $3,436 \text{ cm}^{-1}$ is mainly ascribed to O–H groups on the surface of CuO nanoparticles. The major peak at 533 cm^{-1} reveals the vibration mode of CuO nanoparticles which indicates the formation of CuO nanostructures.

In Fig. 4(c), the peak at 677 cm^{-1} is titanium oxide and refers to the stretching of Ti–O–Ti. The peak at $1,516 \text{ cm}^{-1}$ is due to the lattice vibration of titanium oxide. The bending vibration of coordinated H_2O and

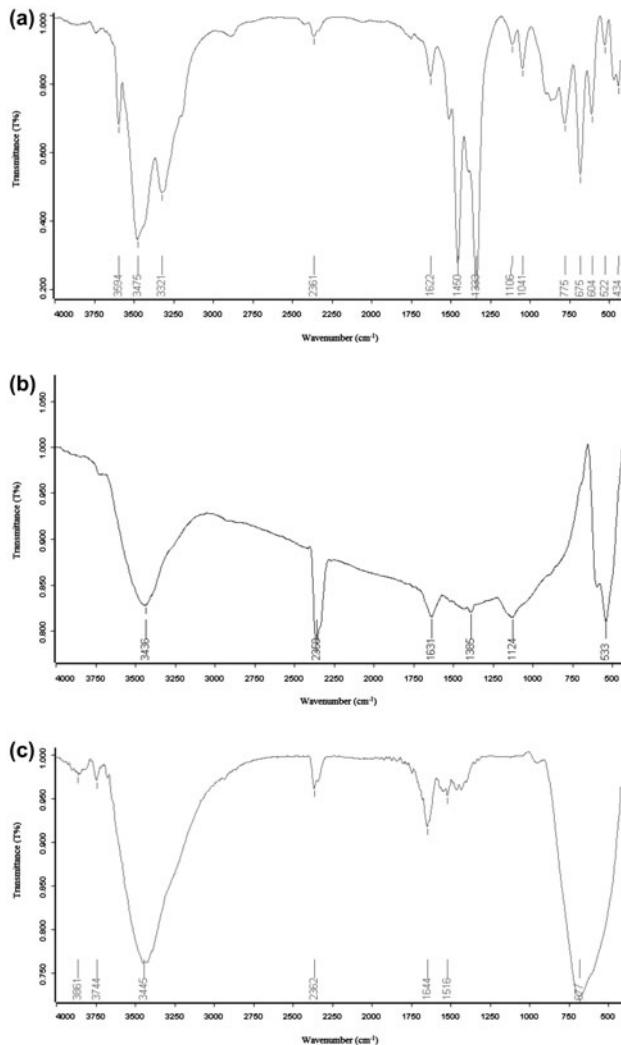


Fig. 4. FTIR pattern of (a) ZnO nanoparticles, (b) CuO nanoparticles, and (c) TiO_2 nanoparticles.

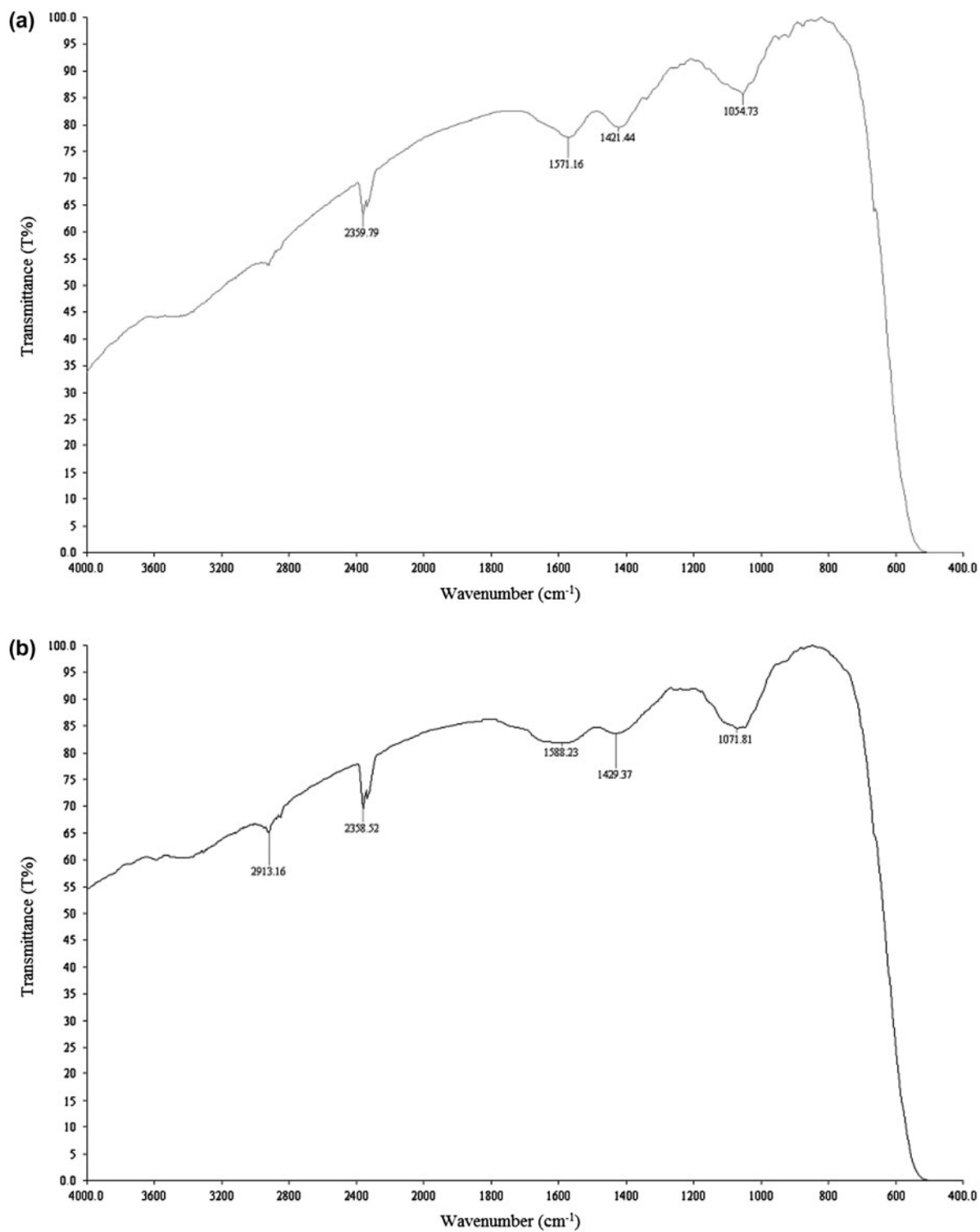


Fig. 5. FTIR pattern of (a) $\text{TiO}_2/\text{ZnO}/\text{CuO}$ nanocomposite from wet impregnation method and (b) $\text{TiO}_2/\text{ZnO}/\text{CuO}$ nanocomposite from mechanical mixing method.

Ti–OH creates the absorbance of $1,644\text{ cm}^{-1}$, and the surface absorbance of water and hydroxyl groups are $2,362$ and $3,445\text{ cm}^{-1}$, respectively.

Fig. 5(a) and (b) shows the FTIR pattern of the nanocomposite from wet impregnation and mechanical mixing, respectively. According to this figure, it is obvious that after the addition of ZnO and CuO to TiO_2 the absorption peak at $2,359\text{ cm}^{-1}$ is due to the surface absorbance of water and hydroxyl group. The absorption peaks at $1,570$, $1,420$, and $1,054\text{ cm}^{-1}$ are due to the existence of TiO_2 , ZnO, and CuO, respectively.

3.1.3. PSA

Fig. 6(a) and (b) shows the particle size distribution of ZnO and CuO samples, respectively. The particle size analyzer (PSA) results show that the size of ZnO and CuO nanoparticles is $<5\text{ nm}$ and 4 nm , respectively, which is appropriate for photo-catalytic applications.

3.1.4. Scanning electron microscopy

The structures of the ZnO, CuO, TiO_2 , the nanocomposites from mechanical mixing, and

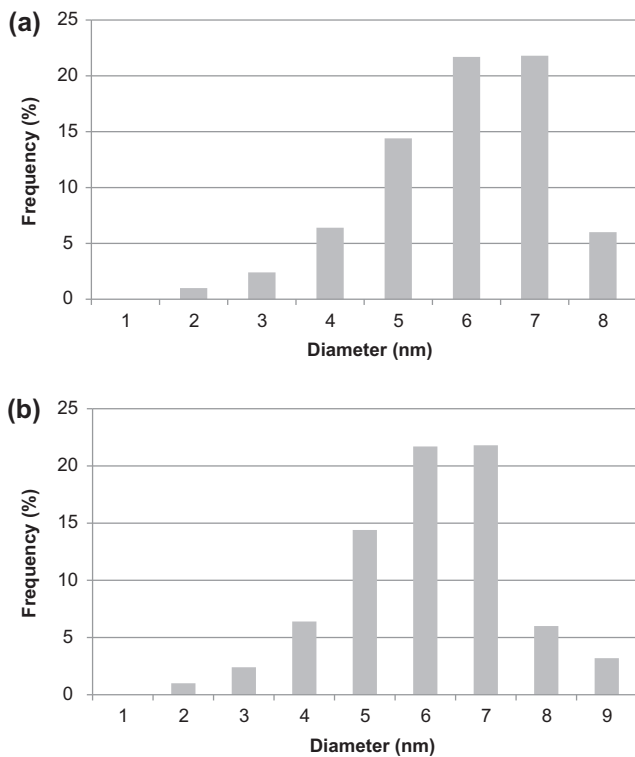


Fig. 6. PSA pattern of (a) ZnO nanoparticles and (b) CuO nanoparticles.

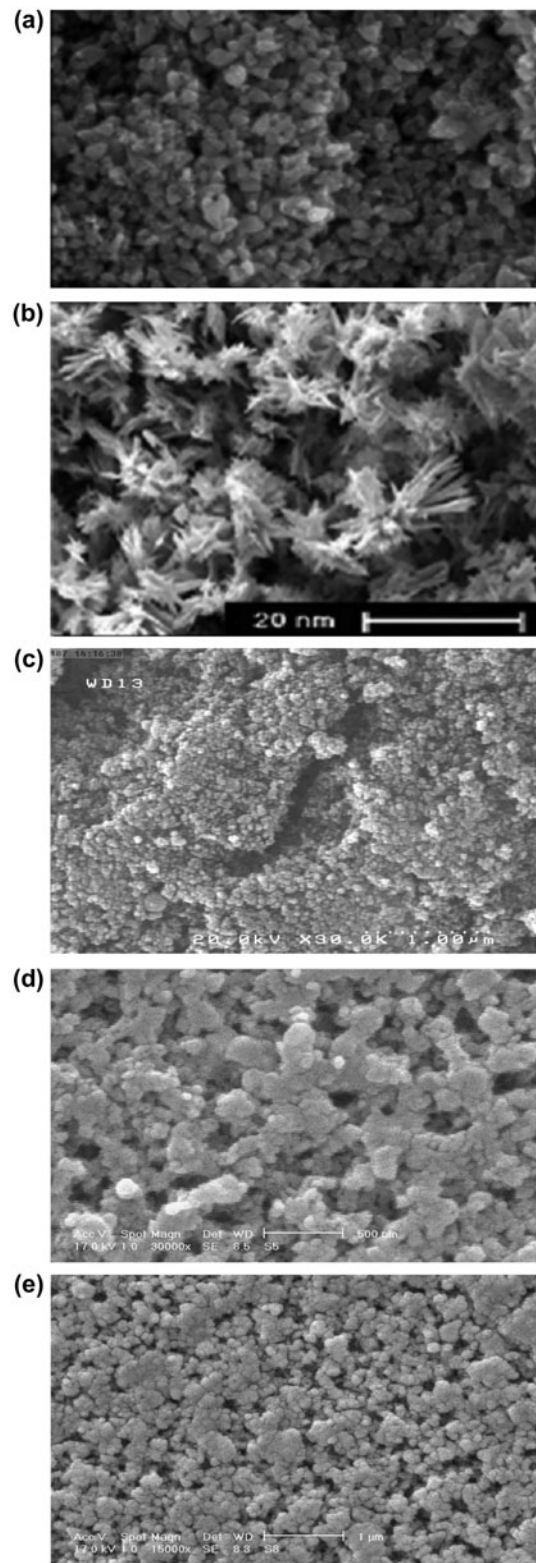


Fig. 7. SEM micrograph of (a) ZnO nanoparticles, (b) CuO nanoparticles, (c) TiO_2 nanoparticles, (d) nanocomposite prepared through mechanical mixing, and (e) nanocomposite prepared through wet impregnation.

Table 1
The optimal pH under UV and solar irradiation using mechanical mixing

pH	Final conc. (ppm)—UV	η (UV) (%)	Final conc. (ppm)—solar	η (solar) (%)
3	21.51	56.98	21.10	49.80
5	19.00	62.00	23.50	53.00
7	26.48	47.04	27.48	45.04
9	29.11	41.78	29.53	40.94
11	30.20	39.60	30.11	39.78

Note: The first concentration is fixed at 50 ppm.

Table 2
The optimum pH value under UV and solar irradiation using impregnation method

pH	Final conc. (ppm)—UV	η (UV) (%)	Final conc. (ppm)—solar	η (solar) (%)
3	20.46	59.08	24.47	51.06
5	17.95	64.00	22.51	54.98
7	25.52	48.96	26.5	47.00
9	28.48	43.04	27.93	44.14
11	29.13	41.48	29.56	40.88

Note: The first concentration is fixed at 50 ppm.

impregnation methods are examined by scanning electron microscopy as illustrated in Fig. 7(a)–(e). It is clear from Fig. 9(b) and (c) that the morphology of the TiO₂/ZnO/CuO nanocomposite is changed completely.

3.2. Degradation of phenol under UV and solar irradiation

3.2.1. The optimization of pH value

The pH of the aqueous solution is a key factor in the photo-catalytic reaction and can affect the adsorption of pollutants onto the photo-catalyst surface. Tables 1 and 2 illustrate the effect of pH on the phenol degradation rate from mechanical mixing and impregnation method, respectively. The degradation rate decreases with increasing pH. The highest degradation efficiency occurs at pH 5 (Tables 1 and 2) which is identical to previous observations [42]. This is attributed to the fact that the produced nanocomposite is amphoteric in aqueous solutions. The point of zero charge is 6.8 for TiO₂ and 8.9 for ZnO and thus, below this value, the nanocomposite surface is positively charged and vice versa. At higher pH values, phenol exists as negatively charged phenolate species. The low degradation rate at higher pH is attributed to the fact that higher OH⁻ concentration prevents the penetration of UV light to reach the catalyst surface. Moreover, high pH value favors the formation of carbonate

ions as effective OH⁻ scavengers leading to the reduction of degradation rate [42].

3.2.2. The optimization of degradation time

The effective application of the photo-catalytic oxidation system requires the investigation of the dependence of photo-catalytic degradation rate on the degradation time. In this section, the effect of degradation time on the degradation of phenol under UV and solar irradiation is examined using the synthesized nanocomposite. The maximum slope in the degradation rate graph was observed during the first 100 min

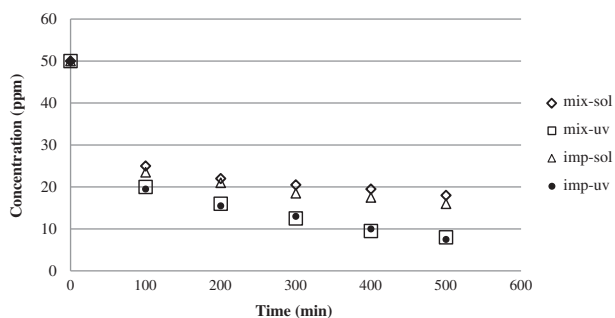


Fig. 8. Time optimization for the synthesized nanocomposites.

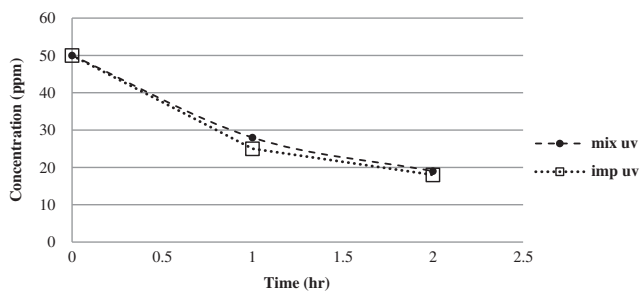


Fig. 9. Nanocomposites under UV irradiation.

(Fig. 8). Thus, it is uneconomical to continue the process in the upcoming moments.

3.2.3. The effect of synthesis method on phenol removal

In this section, the synthesis method and its influence on phenol removal has been investigated. Figs. 9 and 10 show that wet impregnation can be considered as more effective in comparison with mechanical mixing. The reason is that the formation of 3D flower-like $\text{TiO}_2\text{-ZnO-CuO}$ nanocomposite was better performed. In wet impregnation it is well known that the shape of nanocrystals can be controlled by manipulating the growth kinetics [8,9]. In the present case, high amount of TiO_2 led to a burst of initial homogeneous nucleation, and then the supersaturated ZnO nuclei tended to aggregate in order to decrease the surface energy. As the reaction proceeded, the concentration of ZnO and CuO became lower and some active sites on the surface of initially formed ZnO aggregates would grow along on oriented direction. The preferential growth along the oriented directions resulted in ZnO nanoflakes on the surface of the initially formed $\text{TiO}_2\text{-ZnO}$ aggregations [10]. Meanwhile, leaf-like CuO nanopatches grew on the ZnO- TiO_2 aggregations. Subsequently, more and more nanoflakes interlaced and overlapped into a multilayer and network-like structure, and the hierarchical TiO_2 flower-like

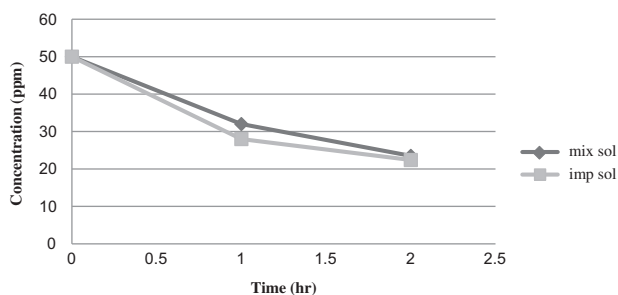


Fig. 10. Nanocomposites under solar irradiation.

microstructures decorated with leaf-like ZnO-CuO nanopatches were shaped. As a result, 3D flower-like ZnO-CuO nanocomposite was prepared in this system.

4. Conclusions

The degradation of phenol is investigated as the model pollutant in industrial waters using the $\text{TiO}_2/\text{ZnO/CuO}$ nanocomposite under irradiation with UV and solar light. The source of UV irradiation was either an 8 W UV lamp or solar radiation. The nanocomposite was prepared by mechanical mixing and impregnation methods. The impregnation method was more effective in comparison with mechanical mixing. The best pH for the degradation of a 50 ppm solution of phenol at 25°C and 0.15 g of nanocomposite was at pH 5. The photo-degradation rate of phenol was found to increase along with increasing pH and then practices a reduction. Using UV-vis spectroscopy, 62 and 53% efficiencies were obtained under UV and solar radiation from mechanical mixing, and 64 and 54.98% efficiencies under UV and solar radiation from wet impregnation, respectively.

References

- [1] M.R. Hoffmann, S.T. Martin, W. Choi, D.W. Bahnemann, Environmental applications of semiconductor photocatalysis, *Chem. Rev.* 95 (1995) 69–96.
- [2] P.D. Cozzoli, E. Fanizza, R. Comparelli, M.L. Curri, A. Agostiano, D. Laub, Role of metal nanoparticles in TiO_2/Ag nanocomposite-based homogeneous photocatalysis, *J. Phys. Chem. B* 108 (2004) 9623–9630.
- [3] T.L. Thompson, J.T. Yates Jr., Surface science studies of the photoactivation of TiO_2 new photochemical processes, *Chem. Rev.* 106 (2006) 4428–4453.
- [4] X. Chen, S.S. Mao, Titanium dioxide nanomaterials: Synthesis, properties, modifications, and applications, *Chem. Rev.* 107 (2007) 2891–2959.
- [5] A.L. Linsebigler, G.Q. Lu, J.T. Yates, Photocatalysis on TiO_2 surfaces: Principles, mechanisms, and selected results, *Chem. Rev.* 95 (1995) 735–758.
- [6] S. Han, S.H. Choi, S.S. Kim, M. Cho, B. Jang, D.Y. Kim, J. Yoon, T. Hyeon, Low-temperature synthesis of highly crystalline TiO_2 nanocrystals and their application to photocatalysis, *Small* 1 (2005) 812–816.
- [7] S.C. Liao, H.F. Lin, S.W. Hung, C.T. Hu, DC thermal plasma synthesis and properties of zinc oxide nanorods, *J. Vac. Sci. Technol., B* 24 (2006) 1332–1335.
- [8] H.G. Kim, P.H. Borse, W. Choi, J.S. Lee, Photocatalytic nanodiodes for visible-light photocatalysis, *Angew. Chem. Int. Ed.* 44 (2005) 4585–4589.
- [9] T. Arai, M. Yanagida, Y. Konishi, Y. Iwasaki, H. Sugihara, K. Sayama, Efficient complete oxidation of acetaldehyde into CO_2 over $\text{CuBi}_2\text{O}_4/\text{WO}_3$ composite photocatalyst under visible and UV light irradiation, *J. Phys. Chem. C* 111 (2007) 7574–7577.

- [10] C.H. Ye, Y. Bando, G.Z. Shen, D. Golberg, Thickness-dependent photocatalytic performance of ZnO nanoplatelets, *J. Phys. Chem. B* 110 (2006) 15146–15151.
- [11] Z. Zhang, C.C. Wang, R. Zakaria, J.Y. Ying, Role of particle size in nanocrystalline TiO₂-based photocatalysts, *J. Phys. Chem. B* 102 (1998) 10871–10878.
- [12] P.R. Shukla, S. Wang, H.M. Ang, M.O. Tadé, Photocatalytic oxidation of phenolic compounds using zinc oxide and sulphate radicals under artificial solar light, *Sep. Purif. Technol.* 70 (2010) 338–344.
- [13] D.D. Dionysiou, A.P. Khodadoust, A.M. Kern, M.T. Suidan, I. Baudin, J.M. Lainé, Continuous-mode photocatalytic degradation of chlorinated phenols and pesticides in water using a bench-scale TiO₂ rotating disk reactor, *Appl. Catal., B* 24 (2000) 139–155.
- [14] N.H. Salah, M. Bouhelassaa, S. Bekkouche, A. Boultii, Study of photocatalytic degradation of phenol, *Desalination* 166 (2004) 347–354.
- [15] H. Ganjidoust, K. Tatsumi, S. Wada, M. Kawase, Role of peroxidase and chitosan in removing chlorophenols from aqueous solution, *Water Sci. Technol.* 34 (1996) 151–159.
- [16] F. Ge, L. Zhu, J. Wang, Distribution of chlorination products of phenols under various pHs in water disinfection, *Desalination* 225 (2008) 156–166.
- [17] S.K. Johnson, L.L. Houk, J. Feng, R.S. Houk, D.C. Johnson, Electrochemical incineration of 4-chlorophenol and the identification of products and intermediates by mass spectrometry, *Environ. Sci. Technol.* 33 (1999) 2638–2644.
- [18] R. Weber, H. Hagenmaier, PCDD/PCDF formation in fluidized bed incineration, *Chemosphere* 38 (1999) 2643–2654.
- [19] D. Chen, A.K. Ray, Photocatalytic kinetics of phenol and its derivatives over UV irradiated TiO₂, *Appl. Catal., B* 23 (1999) 143–157.
- [20] P.K.J. Robertson, Semiconductor photocatalysis: An environmentally acceptable alternative production technique and effluent treatment process, *J. Clean. Prod.* 4 (1996) 203–212.
- [21] O. Carp, C.L. Huisman, A. Reller, Photoinduced reactivity of titanium dioxide, *Prog. Solid State Chem.* 32 (2004) 33–177.
- [22] T. Essam, M.A. Amin, O. El Tayeb, B. Mattiasson, B. Guieysse, Sequential photochemical biological degradation of chlorophenols, *Chemosphere* 66 (2007) 2201–2209.
- [23] M. Bertelli, E. Selli, Reaction paths and efficiency of photocatalysis on TiO₂ and of H₂O₂ photolysis in the degradation of 2-chlorophenol, *J. Hazard. Mater.* 138 (2006) 46–52.
- [24] S. Contreras, M. Rodríguez, F. Al Momani, C. Sans, S. Esplugas, Contribution of the ozonation pretreatment to the biodegradation of aqueous solutions of 2,4-dichlorophenol, *Water Res.* 37 (2003) 3164–3171.
- [25] F.J. Benitez, J. Beltran-Heredia, J.L. Acero, F.J. Rubio, Contribution of free radicals to chlorophenols decomposition by several advanced oxidation processes, *Chemosphere* 41 (2000) 1271–1277.
- [26] M.P. Ormad, J.L. Ovelleiro, J. Kiwi, Photocatalytic degradation of concentrated solutions of 2,4-dichlorophenol using low energy light, *Appl. Catal., B* 32 (2001) 157–166.
- [27] W.F. Jardim, S.G. Moraes, M.M.K. Takiyama, Photocatalytic degradation of aromatic chlorinated compounds using TiO₂: Toxicity of intermediates, *Water Res.* 31 (1997) 1728–1732.
- [28] J. Giménez, D. Curcó, M.A. Queral, Photocatalytic treatment of phenol and 2,4-dichlorophenol in a solar plant in the way to scaling-up, *Catal. Today* 54 (1999) 229–243.
- [29] N.N. Rao, A.K. Dubey, S. Mohanty, P. Khare, R. Jain, S.N. Kaul, Photocatalytic degradation of 2-chlorophenol: A study of kinetics, intermediates and biodegradability, *J. Hazard. Mater.* 101 (2003) 301–314.
- [30] M. Romero, J. Blanco, B. Sánchez, A. Vidal, S. Malato, A.I. Cardona, E.G. Garcia, Solar photocatalytic degradation of water and air pollutants: Challenges and perspectives, *Sol. Energ.* 66 (1999) 169–182.
- [31] O.M. Alfano, D. Bahnemann, A.E. Cassano, R. Dillert, R. Goslich, Photocatalysis in water environments using artificial and solar light, *Catal. Today* 58 (2000) 199–230.
- [32] S. Malato, J. Blanco, A. Vidal, C. Richter, Photocatalysis with solar energy at a pilot-plant scale: An overview, *Appl. Catal., B* 37 (2002) 1–15.
- [33] A.M. Peiró, J.A. Ayllón, J. Peral, X. Doménech, TiO₂-photocatalyzed degradation of phenol and ortho-substituted phenolic compounds, *Appl. Catal., B* 30 (2001) 359–373.
- [34] E. Kusvuran, A. Samil, O.M. Atanur, O. Erbatur, Photocatalytic degradation kinetics of di- and tri-substituted phenolic compounds in aqueous solution by TiO₂/UV, *Appl. Catal., B* 58 (2005) 211–216.
- [35] G. Kumara, F.M. Sultanbawa, V.P.S. Perera, I.R.M. Kottegoda, K. Tennakone, Continuous flow photochemical reactor for solar decontamination of water using immobilized TiO₂, *Sol. Energ. Mater. Sol. Cells* 58 (1999) 167–171.
- [36] K. Wilke, H.D. Breuer, The influence of transition metal doping on the physical and photocatalytic properties of titania, *J. Photochem. Photobiol., A* 121 (1999) 49–53.
- [37] A.G. Agrios, P. Pichat, State of the art and perspectives on materials and applications of photocatalysis over TiO₂, *J. Appl. Electrochem.* 35 (2005) 655–663.
- [38] U.I. Gaya, A.H. Abdullah, Heterogeneous photocatalytic degradation of organic contaminants over titanium dioxide: A review of fundamentals, progress and problems, *J. Photochem. Photobiol., C* 9 (2008) 1–12.
- [39] M. Muruganandham, M. Swaminathan, Photocatalytic decolourisation and degradation of Reactive Orange 4 by TiO₂-UV process, *Dyes Pigm.* 68 (2006) 133–142.
- [40] M. Sahoo, S. Sabbaghi, R. Saboori, Synthesis and characterization of mono sized CuO nanoparticles, *Mater. Lett.* 81 (2012) 169–172.
- [41] J. Zhu, D. Li, H. Chen, X. Yang, L. Lu, Highly dispersed CuO nanoparticles prepared by a novel quick-precipitation method, *Mater. Lett.* 58 (2004) 3324–3327.
- [42] F. Akbal, A.N. Onar, Photo-catalytic degradation of phenol, *Environ. Monit. Assess.* 83 (2003) 295–302.